Payri, R., García-Oliver, J. M., Bardi, M., & Manin, J. (2012). Fuel temperature influence on diesel sprays in inert and reacting conditions. *Applied Thermal Engineering*, *35*, 185-195

Fuel temperature influence on Diesel sprays in inert and reacting conditions

Raul Payri (1)
Jose Maria García-Oliver (1)
Michele Bardi (1)
Julien Manin (2)

(1) CMT-Motores Termicos, Universitat Politecnica de Valencia, Spain
(2) CRF - Sandia National Laboratories

Abstract

The detailed knowledge of the evaporation-combustion process of the Diesel spray is a key factor for the development of robust injection strategies able to reduce the pollutant emissions and keep or increase the combustion efficiency. In this work several typical measurement applied to the diesel spray diagnostic (liquid length, lift-off length and ignition delay) have been employed in a novel continuous flow test chamber that allows an accurate control on a wide range of thermodynamic test conditions (up to 1000 K and 15 MPa). A step forward in the control of the test boundary conditions has been done employing a special system to study the fuel temperature effect on the evaporation and combustion of the spray. The temperature of the injector body has been controlled with a thermostatic system and the relationship between injector body and fuel temperature has been observed experimentally. Imaging diagnostics have been employed to visualize the liquid phase penetration in evaporative/inert conditions and, lift off length and ignition delay in reactive condition. The results underline a clear influence of the injector body temperature on both conditions, evaporative and, in a lesser degree, reactive; finally the physical models found in the literature have been compared with the results obtained experimentally.

Payri, R., García-Oliver, J. M., Bardi, M., & Manin, J. (2012). Fuel temperature influence on diesel sprays in inert and reacting conditions. *Applied Thermal Engineering*, *35*, 185-195

1. Introduction

The importance of the injection process in the global functioning of a direct injection Diesel engine is pivotal [1][2]. Lot of studies have been performed in last decades in order to predict the behavior of the spray and various models have been introduced, either based on physical assumptions or simply interpolating experimental data [1][3][4][5][6]. Nowadays, one of the last challenges of the research is to employ CFD models to simulate break-up, evaporation and combustion processes of Diesel sprays [2][7][8][9]: CFD simulations have shown great potential for studying the behavior of the spray, but until now experimental data are still required to adjust the predictions. Being the aim of CFD simulations to be predictive, the models employed are getting each time more detailed in terms of time and space discretization as well as in the physical description of the phenomena including turbulence simulations (LES and DNS) and more accurate descriptions of the fuel physical properties.

To match this effort, also the tests performed need to improve their accuracy, not only in the analysis of the results itself, but also in the definition of the boundary conditions. In this study, a set of experiments has been performed in a high temperature and high pressure test rig, capable of reaching 15 MPa ambient pressure and 1000 K ambient temperature. The large optical accesses and the wide test session allow studying the spray with high accuracy in a homogeneous temperature and nearly quiescent environment. In this work, different parameters have been varied: ambient temperature, ambient density and injection pressure; moreover, the effect of fuel temperature on the results has been studied. A special device to control the temperature of the injector body has been employed during the tests and the same test matrix has been repeated for three different coolant temperatures. In addition, the temperature along the injector axis has been measured using a thermo-couple fitted inside a “dummy” injector and conclusions about the relationship between fuel temperature at the orifice outlet and coolant temperature have been drawn.

In order to enable the comparison with a CFD simulation, a single-component fuel has been employed (n-dodecane): in fact a wide amount of data about this fuel can be found in the literature [10][11].

The injector employed in this work is based on second generation Common-Rail and corresponds to the injector used in the ECN Working Group. As a matter of focusing the attention on the fundamental behavior of the spray a single-hole axial nozzle has been used; the advantage of this kind of nozzle consists in injecting toward the chamber, eliminating both, the effects and the uncertainties related to the temperature boundary layer close to the walls and the spray-spray interaction. The nozzle internal geometry has been characterized by means of the silicon molding technique [12], the results of this technique provide accurate measurement of the outlet orifice diameter of 0.089 mm with a *k–factor* of *2.1*.

The parametric study performed, with a wide characterization (and variation) of test conditions means to be on one side, a contribution for CFD modelers as a reference for results sensitivity to numerous parameters, and, on the other side, a contribution for experimentalists as demonstration of the impact that injector temperature, not mentioned in most of the tests presented in the literature, can have on the final results.

This present document is divided into six sections including the present introduction; the second part will detail the experimental facility, the control system and the test matrix. After the facilities have been presented, the experimental methodology applied in the different tests is described, focusing on the image processing algorithm and criteria. The results both in non-reacting and in reacting atmosphere are shown in the fourth main section. Then, the results are analyzed and discussed with the support of various theoretical approaches. The general conclusions are detailed in the last section of this paper.

2. Experimental setup

As introduced earlier, the tests have been performed in a high temperature and high pressure test chamber where the thermo-dynamic conditions obtained in a Diesel engine at the time of injection can be obtained with maximum ambient temperature 1000 K and maximum pressure 15 MPa. There are several facilities in the world capable of performing alike [13], but in this case it is possible to obtain in the test chamber nearly quiescent, and steady thermodynamic conditions.

The testing section has three large optical accesses (*128 mm* in diameter) placed orthogonally in order to have a complete view of the injection event. A picture of the combustion chamber is included in Figure 1.

The facility is basically composed of four parts: gas compressors, gas heaters, test vessel, control system. The gas, initially stored in high pressure reservoirs, flows continuously through the test chamber via volumetric compressors. Electrical heaters, placed upstream the test chamber, increase the temperature of the flowing gas up to the selected temperature. The control system is a closed loop PID that adjusts both, the pressure in the chamber and the power of the heater to obtain in the chamber the test conditions required for the test. To improve the temperature homogeneity within the test chamber, the vessel has a double wall configuration: while the external walls have the structural function of supporting the pressure of the inner gas, the thinner internal walls are covered with an insulating layer, and have the function of reducing the heating of the outer shell. The internal walls are also heated by a secondary electrical resistance that surrounds the test chamber: the aim of this heater is to reduce the temperature in-homogeneities within the testing section.

The rig can work in open or closed circuit to test spray evolution either in a standard air atmosphere or with gas mixtures with different O_2 concentration. The chemical composition of the gas in the chamber is permanently measured and can be adjusted adding either air or nitrogen through a reintegration system.

The steady thermodynamic conditions within the chamber allows a better (and easier) control of the test conditions; this fact, together with high test repetition rate, results in a global improved accuracy of the data acquired.

Moreover, a special injector holder has been designed specifically for this work: this device maintains the injector in direct contact with a liquid flowing at controlled temperature. The liquid temperature is controlled by means of a PID system able to feed the liquid at temperatures ranging from 15 to 90°C. In order to study the relationship between the coolant temperature and the temperature of the injected fuel a special injector dummy has been employed: this tool has exactly the same shape as the injector used in the test but it is equipped with a thermocouple that can be located all along the injector axis up to be in contact with the nozzle tip.

3. Experimental methodology

A preliminary test has been done to evaluate the relationship between the temperature of the fuel in the sac T_f and the temperature of the coolant T_c. Then, different measurements have been performed to characterize the Diesel spray: Liquid phase penetration (in evaporative-inert conditions), lift-off length and ignition delay (in reactive conditions). A parametrical study has been performed for all of these measurements, changing different test conditions: ambient temperature, ambient density, injection pressure and coolant temperature. The details of the tests performed are described in the following sections and the test conditions are summarized in Table 1.

3.1 Injector temperature measurements

The relationship between coolant temperature T_c and fuel temperature T_f has been studied using a "dummy" injector with a thermo-couple introduced inside down to the sac. In this work T_c is defined as the set-point of the PID controlling the coolant temperature, which practically coincides with the coolant temperature at the injector holder inlet.

The dummy injector is the same injector type as the one used in the other tests performed in this work, but with some modifications: the orifice has not been drilled in the nozzle, a hole has been drilled axially in the needle and the upstream part has been adapted to insert a thin thermocouple. The thermocouple can slide all along the injector axis until getting in contact with the very tip of the internal region of the nozzle (the sac). A scheme of the injector "dummy" is represented in Figure 2. Even if this device is not able to inject fuel, it can provide important information about the temperature inside the injector body. Moreover, the fuel flow, occurring during the tests with the real injector it is considered to have just a minor impact over the injector temperature, and the fuel temperature will be mainly driven by the temperature of the injector. This is justified by the fact that the tests are performed at low repetition rate (0.3 Hz) and the maximum fuel mass per injection is less than 10 mg: the fuel travel for a relatively long time inside the injector and therefore the heat exchanged between the injector and the fuel flow is consider to have a minor influence on injector temperature. The temperature measurements performed, are considered not only a qualitative measurement but also a good approximation of the real temperature of the injector body at the moment of the injection.

In this preliminary test, the temperature has been measured along the injector axis for the three different coolant temperatures employed in the test matrix. In order to take in account also the effect of the chamber temperature T_{amb} the measurements have been repeated for the two cases studied in the test matrix (820 K and 900 K). The temperature has been measured in different position: moving along the injector axis, and considering the distance *x* as the distance between the thermocouple junction and the injector tip, the temperature has been measured for *x* spanning from 0 (thermocouple touching the injector tip) to 35 mm.

3.2 Liquid phase penetration through Mie scattering

The liquid phase penetration or liquid length (LL) is a measurement commonly performed to characterize the mixing process of the Diesel spray [5]; a simple definition of the liquid length can be given as the distance that the injected fuel has to penetrate in the chamber until its complete evaporation. In several studies on liquid phase penetration available in the literature [1][5][14], the dependence of the liquid length upon different parameters such as ambient temperature, ambient density, injection pressure, nozzle diameter and fuel type can be found. To predict the variation of the liquid length, researchers have also developed theories basing on physical hypothesis, like the model developed by Siebers [16] or the one proposed by Desantes [17]: both of them are based on the hypothesis of mixing-limited vaporization and with relatively simple calculations they are able to predict in accurate way the experimental results. The aforesaid models are interesting for the purpose of this work because they permit drawing a comparison with the tendencies experimentally observed. More details about the models will be given in the next sections.

The technique chosen for visualizing the liquid-phase penetration is Mie scattering with frontal illumination. A sketch of the optical set-up is depicted in Figure 3; a high speed CMOS camera (Photron Fastcam) fitted with a 70 mm f/2.8 lens has been employed to acquire images of the injection event. The region of the spray has been illuminated by a continuous Xenon-arc lamp and the light scattered by the liquid droplets has been collected by the camera.

In the literature several approaches for image segmentation can be found [15]; in this case the methodology described by Siebers in [16] has been used. This method consists in subtracting the background and taking a threshold of 3% of the maximum digital level observed in the core of the spray. This method has proved to be sensible and robust enough for different optical settings and experimental conditions.

Payri, R., García-Oliver, J. M., Bardi, M., & Manin, J. (2012). Fuel temperature influence on diesel sprays in inert and reacting conditions. *Applied Thermal Engineering*, *35*, 185-195

3.3 Stationary lift-off length through OH chemiluminescence

The flame lift-off length (LOL) of Diesel fuel sprays is usually defined as the distance from the injector orifice outlet to the reaction zone stabilization after the time of auto-ignition [18][19][20][18]. This characteristic length of the flame is known to have a significant effect on Diesel combustion [1] because it is strongly related to the flame temperature and the amount of soot produced during the combustion [20]. In this study the effect of the injection parameters together with the effect of the coolant liquid temperature on the lift-off length have been observed.

As shown by Dec in [21], OH chemiluminescence is an excellent marker of the high temperature chemical reaction taking place in Diesel spray combustion and many authors have used this method to measure LOL as long as this zone of the flame is characterized by high chemical activity.

Chemiluminescence is a chemical phenomenon consisting in a light emission due to the decay of a molecule from an exited state OH^* to a lower energy level OH. OH-chemiluminescence has a well defined spectrum that permits identifying the emitting molecule [22]. The spectrum of the light emitted by OH^* decay has its most important peak at 306 nm: to catch this light emission a 310 ± 5 nm interferometric filter has been used. Using this filter allow to visualize OH emissions excluding nearly the totality of the soot incandescence radiation, that at higher wavelengths are normally order of magnitudes over chemiluminescence radiations.

In these measurements an Andor ICCD camera (iStar) fitted with an 100 mm f/2.8 UV lens has been employed. The camera intensifier has been set to its maximum gain value and 0.1 ms gate time. The camera trigger has been synchronized to shutter at 3 ms after the start of the injector energizing (Time ASOE) (corresponding roughly to 2.7 ms after the start of injection (Time ASOI)) in order to observe the stabilized lift-off length. The scheme of the optical layout is represented in Figure 4: Experimental lay-out employed for OH radical visualization .

To determine the position of the LOL in a coherent way at the different test conditions, the methodology described by Siebers in [18] has been followed. This approach calculates the digital level threshold scaling the intensity observed in the reacting area and considers separately the two characteristics lobes upstream the flame; the distance calculated for each lobe before is then averaged to have one single LOL value for each image: this method has demonstrated to be robust to the different test conditions and to have low sensibility to changes in camera setting. The image is divided in two parts along the injector axis. For each half-image the maximum digital level of each x coordinate is calculated (see Figure 5); the curves obtained are characterized by a sharp rise followed by a nearly flat zone. The threshold is obtained dividing by two the digital level reached in this part of the flame, normally called leveling value; finally the LOL for each image is obtained as the mean of the LOL calculated in the two halves of the image.

3.4 Ignition delay through CH chemiluminescence

The natural emission of light of the CH^* radicals has been studied using the methodology described in [14]. From the studies of Dec and Espey [23] about chemiluminescence in diesel flames it has been shown that CH is an excellent marker for the characterization of the Diesel combustion. Its timing and location can give precious information on combustion understanding. In their experiments, CH chemiluminescence appeared to be the fair witness of autoignition. Even if some isolated spots could be detected earlier, the brighter homogeneous chemiluminescence of CH would match the first heat release, where heat release curve attains its minimum due to heat loss from fuel evaporation. This chemiluminescence develops uniformly in the rich leading portion of the Diesel fuel jet. The combustion process ensues with fuel breakdown following the first significant heat release and an eventual first soot formation occurring on the peak of premixed flame. This chemiluminescence lasts in rich areas of the jet during the whole combustion event but it is soon hidden by this early soot radiation that is about 3 orders of magnitude brighter.

Following this methodology an intensified camera has been employed in the same optical configuration employed for the OH chemiliminescence but this time the camera has been fitted with a 450 nm band-pass interference filter. To study the rise of the CH^* emission, the synchronization of the camera has been changed in order to study the time evolution of the combustion event. A time-sweep has been performed to record the first part of the combustion event with 20 µs time step and 5 repetitions per time step.

To process the images obtained in this test, the maximum luminosity of each image have been evaluated calculating the percentile at 99.9% of the digital level of the pixels for each image: an average value of the percentile has been calculated for each time step of the time sweep and the time evolution of this parameter (from now on called $p_{99.9\%}$) has been obtained. The ignition delay has been calculated as the first instant when $p_{99.9\%}$ is above the experimental noise.

4. Results

In this section the results obtained in the different tests are shown together with a description of the technique used to present them.

4.1 Injector temperature measurements

The temperature inside the injector has been measured while the rig was running and the temperature values have been acquired continuously by a data-logger. To present the results, the values obtained in each test condition have been averaged along one minute. In Figure 6, the horizontal dashed line indicates T_c while the temperature along the injector axis measured in the different condition is depicted in continuous line.

The temperature measurements performed inside the injector body have shown that there is a strict relationship between the coolant and the injector tip temperature. In fact the variations in coolant temperature are reflected in nearly the same proportion at the nozzle tip that is in contact with the high temperature gas within the test chamber.

Considering the small quantity of fuel injected (less than 10 mg per injection) and the low test frequency (0.3 Hz), the fuel flow through the injector is considered to have low influence on injector temperature: for this reason the temperature measurements performed in this test are considered a good approximation of the real temperature of the injector body at the moment of the injection.

Geometrical calculations matched with mass flow rate measurements, have shown that the volume of fuel injected during one injection event is contained in all the cases between 0 and 3 mm from the injector tip: considering the relatively long time between two injections (about 3.3 s) and the small quantity of fuel injected, we can assume that the temperature of the fuel injected is equal to the average temperature measured between 0 and 3 mm from the injector tip. This consideration will be used later on for the analysis of the LL and LOL results; from now on, the temperature of the injected fuel will be considered

Payri, R., García-Oliver, J. M., Bardi, M., & Manin, J. (2012). Fuel temperature influence on diesel sprays in inert and reacting conditions. *Applied Thermal Engineering*, *35*, 185-195

equal to the average injector temperature measured in the first 3 mm from the tip and it will be referred as T_f.

It is important to notice that also the chamber temperature has an effect on the tip temperature: it means that maintaining a constant coolant temperature is not enough to control fuel temperature; this fact, if not considered, can lead to confuse the effect of the ambient temperature with the fuel temperature. The effect of ambient density on the injector temperature has also been studied, but its effect appeared to be low in the range of conditions tested. The T_f estimated for all the conditions tested is reported in Table 2.

4.2 Liquid phase penetration

The time-resolved LL evolution obtained for three different coolant temperatures is shown in Figure 7 for one sample test condition (T_g = 900 K, ρ_g = 15.2 kg/m^3 and p_r = 150 MPa). The LL curve can be divided in two parts: the first part is characterized by fast penetration rate, where the three cases do not present any revealing difference; the second part where liquid spray penetration stabilizes at a nearly constant value. In this second part of the injection event, it is evident that the temperature of the coolant fluid influences in a substantial way on the liquid length penetration. In particular, it is clear that a higher temperature of the coolant causes the liquid length to decrease. This fact seems to be logical, if we consider that if the injected fuel is hotter when it enters in the chamber, the heat it needs to evaporate is lower and then, it evaporates faster. In order to have a representative value of LL, for each test condition, a mean value of LL has been defined, LL_m , that is the average of the values measured in the interval from 2800 to 3200 μs after start of injection. In Figure 7, the time window employed for the *LL* averaging is represented.

In Figure 8, and Figure 9 the effect of the different test conditions is shown by plotting the LL_m as function of ambient density, ambient temperature and injection pressure for the three different Tf. The standard deviation obtained for the fifteen repetitions performed per each test is always between 0.1-0.8 mm.

4.3 Lift-off length

In Figure 10 and Figure 11, the LOL measurements performed in the tests are depicted. The points indicate the average of fifteen repetitions. To ease the understanding of the results, the experimental standard deviation has been plotted together with the mean value. The parameters which affect LOL the most are ambient temperature and ambient density; injection pressure impact is more significant than in the case of liquid length because LOL is strictly related with fuel velocity at the orifice outlet (this issue will be discussed later). Fuel temperature in this case has only a secondary effect and in some case is below the experimental uncertainty; however the general trend is a small decrease in LOL when T_f is increased. Comparing the results of LOL with LL measurements it can be noticed that LOL is always longer than LL measured in the same test conditions: this fact means that there is no interaction between combustion and evaporating process.

4.4 Ignition delay

As commented above, images of CH* chemiluminescence have been processed by analyzing the 99.9% digital level percentile of all the pixels of each image. In Figure 12, the evolution of the percentile calculated for the images captured during the first part of the combustion has been plotted. The shape of these curves is characterized by a first small hill, followed by a steep increase. The first hill is probably linked to the first premixed combustion that characterizes Diesel flame. After this, soot emissions rise and cover the CH* chemiluminescence emissions, leading the camera sensor to saturate.

The first “hill” appears to be dependent on injection pressure: the higher the injection pressure, the higher the peak value. This fact is in accordance with the previous hypothesis: fuel mass injected during the ignition delay at higher injection pressure is higher and this should result in an increase of the combustion during the premixed flame.

In this study the Ignition delay, has been defined as the first instant in which the percentile calculated is above the experimental noise. With this criterion, the ignition delay has been calculated for all the test conditions. In Figure 13 and Figure 14, the ignition delay has been plotted respectively versus the ambient density and injection pressure.

High temperature and high pressure as seen in LOL results enhance the combustion process reducing the lift off length: this fact is also reflected in the ignition delay. Increasing ambient temperature and ambient density ignition delay decreases significantly. Injection pressure has only a secondary effect, but still it is evident how increasing injection pressure the ignition delay becomes shorter. Ignition delay shows even

Payri, R., García-Oliver, J. M., Bardi, M., & Manin, J. (2012). Fuel temperature influence on diesel sprays in inert and reacting conditions. *Applied Thermal Engineering*, *35*, 185-195

lower sensitivity to T_f: the overall trend observed, is a slight decrease in ignition delay when T_f is increased.

5. Discussion

5.1 Liquid phase penetration

The average liquid phase penetration (LL_m) measured in the tests, shows all the general trends normally observed in the literature [1]. In this study, the theoretical model developed by Desantes et al.[24], is used as a reference. The model is specific for direct injection diesel spray, characterized by high injection pressure (over 40 MPa) and small outlet orifice (less than 0.2 mm) and it is based on the hypothesis of mixing controlled vaporization: in other words, the heat exchange between entrained air and fuel droplets is so fast that is considered to be infinite, and the fuel evaporation is solved as a quasi-steady energy balance between fuel and entrained air. In this way, liquid penetration is calculated as the location where the energy supplied by the entrained air, is enough to vaporize all the fuel. This balance corresponds to a specific fuel mass fraction named $Y_{f,evap}$. The equation describing the liquid length has been derived by previous studies concerning the spray mixing theory developed in [16] [17]. LL is then analytically described as below:

$$LL_m = K\sqrt{C_a}\, d_0 \sqrt{\frac{\rho_f}{\rho_{amb}}} \cdot \frac{1}{Y_{f,evap}} \qquad (1)$$

Where d_o is the orifice diameter, ρ_f and ρ_{amb} are the fuel and air density and C_a is the area coefficient. *K* is a constant depending on the spreading angle:

The last term in equation (1), takes into account the energy needed for the fuel evaporation and physically is the fuel-air mass fraction at which all the fuel is vaporized. $Y_{f,evap}$ can also be written as function of variation of the specific enthalpy of the fuel and of the air. The expression considering the initial condition (T_f and T_{amb}) and the equilibrium temperature of evaporation (T_{evap}) can be written as below

$$\frac{1}{Y_{f,evap}} = 1 + \frac{\Delta h_f\left(T_f, T_{evap}\right)}{\Delta h_a\left(T_{amb}, T_{evap}\right)} \qquad (2)$$

Payri, R., García-Oliver, J. M., Bardi, M., & Manin, J. (2012). Fuel temperature influence on diesel sprays in inert and reacting conditions. *Applied Thermal Engineering*, *35*, 185-195

Where Δh_f and Δh_a are respectively the fuel and air enthalpy variations from the initial temperature (T_f for the fuel, T_{amb} for the ambient gas) to the evaporation temperature T_{evap}. As seen in the experimental results, LL_m is affected mainly by the ambient density and the ambient temperature and, as expected, when ambient density or ambient temperature increase, LL becomes shorter. On the other hand, the model does not include the influence of the injection pressure that appears in the experimental results: a slight decrease in the LL is observed when injection pressure increases. One possibility might be that the spray cone angle ϑ increases with the injection pressure: this fact would affect the constant K of equation (3)

$$LL_m = K\sqrt{C_a}\,d_o\sqrt{\frac{\rho_f}{\rho_{amb}}}\cdot\frac{1}{Y_{f,evap}} \tag{3}$$

and the trend observed would be explained. Unfortunately, other measurements are required to have information about ϑ.

Concerning the influence of the injector temperature two important conclusions can be drawn: first, the effect of the temperature of the injector coolant on *LL* is evident: in fact, the same tendency is observed in each test condition. Moreover, its influence on liquid length is up to 15 % from case Tf = 15 °C to case Tf = 70 °C Thus, if the aim of the experiment is to give quantitative results to be used for modeling, controlling this parameter is fundamental.

In order to have a quantitative evaluation of the trend observed, the model described above has been employed; the effects of the ambient density and fuel temperature have been compared to model predictions. In order to study the influence of ambient density, the relationship between cone angle θ, and ρ_{amb} should be known. Semi-empirical scaling law for the cone angle prediction can be found in the literature [25][26][27], but the results obtained seems to depend strongly on the imaging technique employed and the criterion used for the angle calculation. In conclusion, these equations are not able to predict accurately the cone angle without a calibration with experimental data. However, the impact of the

Payri, R., García-Oliver, J. M., Bardi, M., & Manin, J. (2012). Fuel temperature influence on diesel sprays in inert and reacting conditions. *Applied Thermal Engineering*, *35*, 185-195

ratio of the densities (ambient gases and fuel) has been observed by several and the following proportionality can be written:

$$\tan(\theta/2) \propto \left(\rho_{amb}/\rho_f\right)^a \qquad (4)$$

On the other hand, the exponent a varies in a relatively wide range ($a = 0.18 - 0.50$). As explained before, the spreading angle is related to ambient and fuel density (and thus, fuel temperature), but specific measurements are required to adjust exponent a. In this case, as values of the spreading angle are not available, the model has been tuned adjusting input parameter θ, to match the experimental result only for a reference case ($T_{amb} = 900\,K, \rho_{amb} = 22.8\,{kg}/{m^3}, T_c = 343\,K, p_{rail} = 150\,MPa$); for different ρ_{amb} the cone angle used has not been changed. As expected, in the comparison depicted in Figure 15, the model, as consequence in not considering variations in cone angle, clearly under-predicts the effect of ambient density on LL. However, it can be noticed that the variations predicted are about half the variations experimentally observed: one possible interpretation of this result, is that the variation in LL due to the ambient density is balanced between the changes in the thermodynamic characteristics of the air entrained in the spray and changes of the spray shape.

The influence of T_{amb} experimentally observed has been compared with model predictions, tuning the model at three different ambient density at T_{amb} = 900 K and then, comparing experimental data and predictions at T_{amb} = 820 K. The comparison shows very good agreement between experimental and theoretic predictions.

As in the previous case, the effect of T_f observed, is compared with model predictions. In equation 2 can be seen how fuel temperature appears in the law: it is important to notice that the effect of T_f is just linked with the starting enthalpy of the fuel and thus to the amount of air to be entrained for the evaporation of the spray. To exclude all the other deviation between the model and experimental results, the model has been tuned to the experimental datum of liquid length at T_c = *343 K* for each test condition and only the tendency regarding the fuel temperature has been investigated. In Figure 16, a comparison of the model and the experimental results is presented. For the results related to T_f = *343 K,* the model and experimental data overlap as long as the model has been calibrated on these datum. In the case T_f = *293*

Payri, R., García-Oliver, J. M., Bardi, M., & Manin, J. (2012). Fuel temperature influence on diesel sprays in inert and reacting conditions. *Applied Thermal Engineering*, *35*, 185-195

K and T_f = *318 K,* the comparison put in evidence a good agreement between the prediction and the experimental observations: the model is able to catch the trend and the order of magnitude of the variations due to the change in fuel temperature. However, it is important to point out that the model normally under-predicts the influence of T_f. The cause of this deviation is not clear but one possible reason can be the fact that the model does not take in account the variation of the physical property of the fuel in the liquid phase such as kinematic viscosity and surface tension: these physical properties are known to have a key role in the spray brake up process and then in the air entrainment [28][30] [29]. One other insight can be found in equation (3):ϑ depends upon the fuel density ρ_f. Following this reasoning increasing in fuel temperature causes the spray cone angle to decrease and then, LL to increase.

Finally, with the aim of giving a quantitative description of the trends experimentally observed a statistical analysis on the parameter varied in the test matrix, has been performed; a regression to the data has been done using the equation below:

$$LL \propto \rho_f^{0,5} \cdot \rho_g^b \cdot T_g^c \cdot T_f^d \cdot \Delta p^e \qquad (5)$$

All the exponents in equation (5) has been adjusted to have the best fit to the experimental data. The fuel density ρ_f used for the calculation has been obtained from the NIST database considering backpressure and fuel temperature; the temperature of the fuel at the orifice outlet T_f, as mentioned above, has been considered to coincide with the average injector temperature measured in the first 3 mm from the injector tip in the correspondent test conditions. In this way, the changes in ρ_f in the test matrix due to changes in fuel temperature, have been taken into account. Finally, the statistical parameter R^2 has been calculated and the results are shown in Table 3.

The high value obtained for the statistical parameter R^2 suggests a high precision of the experiment due to both the test rig and the diagnostic applied. Moreover, it is interesting to observe that there is, in general, good agreement between the theoretical and the *best-fit* exponent, calculated for $\rho_a$and ρ_f.

Payri, R., García-Oliver, J. M., Bardi, M., & Manin, J. (2012). Fuel temperature influence on diesel sprays in inert and reacting conditions. *Applied Thermal Engineering*, *35*, 185-195

5.2 Lift-off length

The results obtained indicate that the parameters mainly affecting LOL are the ambient temperature, ambient density and injection pressure. As seen in previous works [1][4][18][19], an increase in ambient temperature or gas density causes a decrease in LOL; on the other hand an increase in injection pressure cause longer LOL: this fact can be explained using two different approaches:

- Considering the gas-jet theory describe by Peters in [20], the lift-off is considered as the distance from the tip where there is equivalence between the velocity of the fuel jet, and the flame front speed. Using this approach an increase in injection pressure affects the LOL because the increase in fuel velocity moves forward this equilibrium distance.
- Another approach to consider LOL has been discussed by Pickett and coworkers in [31]. In this work, LOL is related with ignition delay, and it is described by the Arrhenius-type law. Thus, the Lift-off length is considered as the distance that the fuel travels before the high temperature reactions start. At higher injection pressure during ignition delay, the fuel will travel more distance, and consequently lift-off length will result longer.

In both the approaches, as discussed for liquid length, the heat exchange between droplets and entrained air is considered to be infinite and the problem is solved as a quasi-steady energy balance between fuel and entrained air.

In order to compare the effect of the parameters observed, with what is described with the theory, a comparison with the prediction of the scaling law derived by Peters has been drawn. The scaling law is based on the hypothesis of gas jet behavior of the Diesel spray and it is described in [17]. Peters reviewed much of the experimental gas-jet flame lift-off investigations and analytically derived a scaling law for lift-off length that is in agreement with the experimental trends observed for gas-jets. The scaling law was derived observing that the lift-off length stabilizes in a thin region very close to the stoichiometric contour, and making the hypothesis that the Damköhler number is of order of one at the stabilization location, that means that the local flame reaction rate is comparable to the local mixing rate; this law has shown to predict reasonably the Diesel flame behavior also in other works like in the Lift-off length characterization carried out by Siebers in [18]. The scaling law proposed by Peters is reported in equation (6):

Payri, R., García-Oliver, J. M., Bardi, M., & Manin, J. (2012). Fuel temperature influence on diesel sprays in inert and reacting conditions. *Applied Thermal Engineering*, *35*, 185-195

$$LOL = \frac{u_{eff} Z_{st} \ D}{s_L^2 (Z_{st})} \quad (6)$$

Where u_{eff} is the effective velocity at the exit of the orifice, Z_{st} the stoichiometric fuel mixture fraction, *D* is the thermal diffusivity and $s_L(Z_{st})$ is the laminar flame speed at stoichiometric fuel-air mixture.

$s_L(Z_{st})$ for hydrocarbons has an analytic expression usually of the form:

$$s_L(Z_{st}) = s_{L0} \cdot \left(\frac{T_{mix}}{298K} \right)^{\alpha} \cdot \left(\frac{p_{amb}}{1atm} \right)^{\beta} \quad (7)$$

Where T_{mix} and p_{amb} are the temperature and the pressure of the air-fuel mixture and s_{L0} is the laminar flame speed at reference thermo-dynamic conditions (T_{mix} = 298 K and p_{amb} = 1 atm). The exponents α and β are dependent on the hydrocarbon properties. However the variation of these coefficients is limited, and as long as they are not available in the case of n-dodecane, following the approach used by Siebers in [18] the following coefficients have been employed: α = 2,1 and β = -0,36.

Substituting equation (2) in equation (1) and considering the dependence upon temperature and ambient density of the thermal diffusivity of a gas the scaling law can be written like below:

$$LOL \propto T_{mix}^{-3.7} \cdot \rho_{amb}^{-0,8} \cdot u_{eff}^{1} \quad (8)$$

Following the same approach, T_{mix} will be considered equal to the ambient temperature. The analysis has been performed in two cases: in case I the exponent provided by the theory has been used. In case II the exponent will be adjusted in order to have the best fit to the experimental data. Moreover, to take into account the effect of T_f in T_{mix}, T_f was analyzed as a separate term in equation 8. Equation 8 is re-written in the form below:

$$LOL \propto T_{amb}^{a} \cdot \rho_{amb}^{b} \cdot u_{eff}^{c} \cdot T_f^{d} \quad (9)$$

The effective velocity is dependent on the pressure drop across the orifice and it is obtained experimentally, in the same way as the area coefficient C_a mentioned before, in the hydraulic characterization of the injector.

The results presented in Table 4 show a reasonable agreement between theory and experimental results for the dependence of temperature and ambient density. The exponent obtained for ambient density and ambient temperature are reasonably close. The dependence on the effective velocity is quite different (0,52 instead of the theoretical value 1). A possible reason can be linked to a variation of the angle increasing the injection pressure; this would also be consistent with the reduction in liquid length observed while increasing the injection pressure. Also in this case, the high value of the R^2 obtained with the best fit remarks the precision of the test rig and the robustness of the diagnostic applied.

Focusing on the influence of the coolant temperature LOL, the results shows only a slight dependence and in most of the cases is of the same magnitude of the standard deviation. However, also if the effect is very low, this tendency can be explained through the non-premixed gas-jet theory by Peters mentioned before. In fact, the hypothesis of equality between the mixture temperature T_{mix} and ambient temperature T_{amb} does not consider the effect that the fuel has on the mixture. In order to relate the effect of the fuel temperature on the mixture temperature, the energy balance between the liquid fuel and the hot gas in the chamber has been resolved. In the same way as before, considering the fuel temperature to be the equal to the tip temperature measured with the injector dummy, and considering the adiabatic gas-fuel mixing, the variation of the stoichiometric mixture temperature caused by different fuel temperatures has been obtained. These calculations have shown that a variation of fuel temperature of 25 K can cause variations in the mixture temperature of 2-3 K that are reflected in LOL variation of 1-1.5%. This variation of the same order of magnitude of what has been observed experimentally but still the experimental incertitude does not allow to go further in the conclusions. The effect of T_f on the stoichiometric mixture temperature can be observed in Figure 18. The same figure shows how T_f has a different impact on the mixture temperature at LL and LOL region: for the two exptre cases of T_f the difference in mixture temperature is one order of magnitude higher at fuel mass fraction correspondent to the liquid length, than at the stoichiometric fuel-mass fraction correspondent to LOL region.

5.3 Ignition delay

Ignition delay results obtained by means of chemiluminescence, have shown good coherence in the entire test matrix. Also in this case, results appear to be qualitatively logical: the temperature and the ambient density have the effect to reduce the ignition delay. A weak dependence on injection pressure can be appreciated, too. In this case, the influence of the fuel temperature cannot be observed clearly, and the eventual effect is covered by the experimental incertitude.

In the literature, lots of authors has described the ignition delay by means of empirical correlation. A review of them has been presented by Heywood [32] and Ramos [7]. Some authors like Stringer [33] or Hiroyasu [34] have derived an Arrhenius type expression including the effect of chamber temperature, ambient pressure and the characteristics of the fuel, but without including the injection pressure. As experimentally observed by other authors [4][19][31], injection pressure is strictly linked with ignition delay: this effect has been taken into account in the equation derived by Pischinger that in [35]. The equation is reported below:

$$\tau \propto {P_{back}}^{n} \cdot \exp\left(\frac{E_A}{R \cdot T_{amb}}\right) \cdot \Delta P^{m} \tag{10}$$

Where τ is the ignition delay, P_{back} is the pressure in the combustion chamber, E_A is the activation energy, R the universal gas constant and ΔP is the fuel pressure drop along the injector orifice. To simplify the statistical analysis the terms $\frac{E_A}{R}$ will be renamed as A, a parameter calculated in the regression. The equation can be rewritten as below:

$$\tau \propto {P_{back}}^{n} \cdot \exp\left(\frac{A}{T_{amb}}\right) \cdot \Delta P^{m} \cdot T_f^{a} \tag{11}$$

The results obtained in the regression have been compared as reference to the coefficient obtained in a similar study in [4][1]. The results of the analysis are shown in Table 5. It has to be noticed that the R^2 calculated in the regression presents an important discrepancy: this fact is not surprising as long the parameter A is dependent also on the activation energy that is dependent on the fuel employed and in [3][4][1] a different fuel has been used (Repsol CEC RF-06-99 instead of n-dodecane). Apart from this difference, it is important to note that keeping the other coefficient and adjusting the dependence on the fuel temperature, the R^2 found is very high (98,8%). This means that, despite the experimental incertitude, the effect of fuel temperature on the ignition delay is captured by the statistical analysis. However, the

Payri, R., García-Oliver, J. M., Bardi, M., & Manin, J. (2012). Fuel temperature influence on diesel sprays in inert and reacting conditions. *Applied Thermal Engineering*, *35*, 185-195

overall impact of T_f on ignition delay is low (about 1%, depending on the test conditions): following the same line of argument used for LOL, in the region where the combustion starts the fuel air ratio is lower than at the LL distance: for this reason the temperature of the fuel has a lower weight on the thermodynamic conditions determining the combustion timing and thus on ignition delay.

6. Conclusions

A parametrical study on the liquid phase penetration, lift off length and ignition delay has been carried out in a novel high temperature high pressure test rig. The parametrical study included variation in ambient temperature, ambient density, injection pressure and a specific study on the sensibility of the measurements to the fuel temperature. The study has been carried out with a mono-orifice 90 µm diameter nozzle injector using a mono-component fuel (n-dodecane). The test conditions employed are typical of Diesel engines using moderate level of EGR.

The results obtained in the different tests have been analyzed and tendencies observed have been compared to results presented by other authors. The following general conclusions can then be drawn:

- The results obtained in all the tests show great precision of the test rig and coherence in the entire test matrix. Also, the experimental error observed appears to be low and in most of the cases all the modifications in the test conditions can be observed in the results.
- A specific new device has been employed to control the temperature of the fuel: the tests have been repeated for different coolant temperatures and the relationship between the fuel temperature and the coolant temperature have been obtained by means of direct measurements with injector dummy.
- The comparison with the correlations found in the literature has shown in all the cases good agreement with the trend observed. In this analysis data obtained in the hydraulic characterization of the injector, have been used.
- One exception to the previous sentence is the dependence of the LOL on the effective velocity u_{eff} (the exponent presented by Siebers and Higgins in [18] is $c=1$, while the exponent calculated for the best fit is $c=0{,}52$). A possible reason can be linked to a variation of the angle

with the injection pressure; this would also be consistent with the reduction in liquid length observed increasing the injection pressure.

- The consistency between the data obtained in these tests with the data found in the literature suggests that the novel combustion vessel, with higher repetition rate than other facilities (100 times more than a constant volume combustion vessel) and high flexibility in the test conditions is a powerful tool for future research on Diesel spray.
- The effect of the fuel temperature is substantial on liquid length (up to 15%), and very low but still appreciable on LOL and ignition delay.
- In the case of LL the influence of the fuel temperature has been compared with the prediction of the model presented by Desantes et al. based on mixing limited vaporization: the model catches the influence of the fuel temperature but seems to underestimate the effect. This fact is probably due to both of the following reasons: the model does not take into account the variation due to the temperature of some physical proprieties of the fuel (surface tension and cinematic viscosity); the variation of fuel density related to variations is fuel temperature may cause variations in the cone angle.
- In the case of LOL, the influence of fuel temperature has been justified theoretically with the Peters scaling law and the predictions are in reasonable agreement with the experimental observations.
- Future works should be addressed to the understanding of eventual fuel temperature variation taking place during the expansion in the orifice: the authors consider that the fuel expansion (the fuel cannot be considered incompressible at pressures over 100 MPa) and the fluid friction with the orifice's walls can cause further variation in the fuel temperature.

Acknowledgements

This research has been funded in the frame of the project FLEXIFUEL reference TRA2010-17564 from Ministerio de Ciencia e Innovación. The injectors are part of the ECN international project.

Payri, R., García-Oliver, J. M., Bardi, M., & Manin, J. (2012). Fuel temperature influence on diesel sprays in inert and reacting conditions. *Applied Thermal Engineering*, *35*, 185-195

Bibliography

[1] Soid S. N.; Zainal Z. A., Spray and combustion characterization for internal combustion engines using optical measuring techniques - A review, ENERGY, Volume: 36 (2), pp 724-741, 2011

[2] Hocine, A., Desmet, B., Guenoun, S., Numerical study of the influence of diesel post injection and exhaust gas expansion of the thermal cycle of an automobile engine, Applied Thermal Engineering, Vol 30, pp. 1889-1895, 2010

[3] Payri, R., Salvador, F.J., Gimeno. J., De la Morena, J., Influence of injector technology on injection and combustion development – Part 1: Hydraulic characterization, Appl. Energy, pp. 1068-1074, 2011

[4] Payri, R., Salvador, F.J., Gimeno. J., De la Morena, J., Influence of injector technology on injection and combustion development – Part 2: Combustion analysis, Appl. Energy, Vol 88 (4), pp. 1130-1139, 2011

[5] Siebers D.L., Liquid-Phase Fuel Penetration in Diesel Sprays, SAE Paper 980809 (1998)

[6] Myong K, Arai M, Suzuki H, Senda J, Fujimoto H., Vaporization Characteristics and Liquid-Phase Penetration for Multi-Component Fuels, SAE 2004-01-0529 (2004)

[7] Ramos, J., Internal combustion engine modelling, Hemisphere publishing corporation, ISBN 0-89116-157-0, 1989

[8] Salvador, F.J., Martínez-López, J., Romerob, J.-V., Roselló, M.-D., Influence of biofuels on the internal flow in diesel injector nozzles, Mathematical and Computer Modelling, Elsevier, 2010

[9] Som, S Ramirez, AI Longman, DE Aggarwal, SK., Effect of nozzle orifice geometry on spray, combustion, and emission characteristics under diesel engine conditions, FUEL 90 (3), pp. 1267-1276, 2011

[10] Lawrence Livermore National Laboratory, Physical and Life Sciences Directive. www-pls.llnl.gov/?url=science_and_technology-chemistry-combustion-c8c16_n_alkanes, last access September 2011

[11] Som, S Aggarwal, SK El-Hannouny, EM Longman, DE, Investigation of Nozzle Flow and Cavitation Characteristics in a Diesel Injector, JOURNAL OF ENGINEERING FOR GAS TURBINES AND POWER-TRANSACTIONS OF THE ASME, Vol 132 (4), 2010

[12] Macián, V., Bermúdez, V., Payri, R., Gimeno, J., New technique for determination of internal geometry of a Diesel nozzles with the use of silicone methodology, Exp. Techniques; vol. 27, pp. 39-43, 2003.

[13] Baert, R., Frijters, P., Somers, B., Luijten, C., Design and operation of a high pressure, high temperature cell for HD diesel spray diagnostics: guidelines and results," SAE Paper 2009-01-0649, 2009

[14] Pastor J.V., Payri, R., Gimeno J., Nerva J.-G., Experimental Study on RME Blends: Liquid-Phase Fuel penetration, Chemiluminescence, and Soot Luminosity in Diesel-Like Conditions, Energy Fuels 2009, 23, 5899–5915

[15] Macian, V.,Payri, R., Garcia, A., Bardi, M., Experimental Evaluation of the Best Approach for Diesel Spray Images Segmentation, Experimental Technique, 2011

[16] Siebers, D.L., Scaling liquid-phase fuel penetration in Diesel sprays based on mixing-limited vaporization –SAE-1999-01-0528

[17] Pastor, J.V., Lopez, J.J., Garcia-Oliver, J.M., Pastor, J.M. A 1D model for the description of mixing-controlled inert diesel sprays, Fuel, Volume 87, Issues 13-14, October 2008, Pages 2871-2885

Payri, R., García-Oliver, J. M., Bardi, M., & Manin, J. (2012). Fuel temperature influence on diesel sprays in inert and reacting conditions. *Applied Thermal Engineering*, *35*, 185-195

[18] Siebers. D.L., and Higgins B.S. Flame Lift-Off on Direct-Injection Diesel Sprays Under Quiescent Conditions, SAE 2001-01-0530, 2001.

[19] Payri R. and Salvador F.J. and Gimeno J. and de la Morena J., Effects of nozzle geometry on direct injection diesel engine combustion process. Applied Thermal Engineering, vol. 29, pp. 2051-2060, 2009.

[20] Peters, N., Turbulent Combustion, Cambridge University press, Cambridge UK, 2000

[21] Dec, J.E.; Coy, E.B., Radical imaging in a direct Diesel engine and structure of the early diffusion flame. SAE paper 960831, 1996

[22] Gaydon, A.G., the spectroscopy flames, 2nd ed; FRS Chapman & Hall; London UK, 1974.

[23] Dec, J.E. and Espey, C., Chemiluminescence Imaging of Autoignition in a Di Diesel Engine, SAE Paper 982685, 1998.

[24] Desantes, J.M., Pastor, J.V., Garcia-Oliver, J.M., Pastor, J.M. A 1D model for the description of mixing-controlled reacting diesel sprays, Combustion and Flame, Volume 156, Issue 1, Pages 234-249, 2009

[25] Reitz, R. and Bracco, F., On the dependence of spray angle and other spray parameters on nozzle design and operating conditions. SAE Paper 790494, 1979.

[26] Ruiz, F. and Chigier, N.A., Parametric experiments on liquid jet atomization spray angle. Atomization and Sprays, vol. 1, pp. 23-45, 1991.

[27] Martinez-Martinez, S. and Sanchez-Cruz, F.A. and Riesco-Avila, J.M. and Gallegos-Munoz, A. and Aceves, S.M., Liquid penetration length in direct diesel fuel injection. Applied Thermal Engineering, vol. 28, pp. 1756-1762, 2008.

[28] Desantes, J.M. and Payri, R. and Garcia, A. and Manin, J., Experimental Study of Biodiesel Blends' Effects on Diesel Injection Processes. Energy & Fuels, vol. 23, pp. 3227-3235, 2009.

[29] Payri, R., Salvador, F.J., Gimeno, J., de la Morena, J., Effects of nozzle geometry on direct injection diesel engine combustion process Applied Thermal Engineering, Vol 29 (10), pp. 2051-2060, 2009

[30] Payri, R., Salvador, F.J., Gimeno, J., Bracho, G., The effect of temperature and pressure on thermodynamic properties of diesel and biodiesel fuels, FUEL, vol. 90, pp. 1172-1180, 2011.

[31] Pickett, L.M., Siebers, D.L., Idicheria, C.A., Relationship between ignition process and the Lift-Off Length of Diesel Fuel Jets, SAE 2005-01-3843, 2005.

[32] Heywood, J., Internal combustion engine fundamentals, Mc. Graw-Hill, New York, US, ISBN 0-07-028637-X, 1988

[33] Stringer, F.W., Clarke, A.E., Clarke, J.S., The spontaneous ignition of hydrocarbon fuels in a flowing system", Proc. Instn Mech Engrs., vol. 184, 1969-1970.

[34] Hiroyasu, H., Kadota, T., Arai, M., Supplementary coments: fuel spray characterization in Diesel engines, Combustion modeling in Reciprocating Engines, pp. 369-408, 1980.

[35] Pischinger, F., Reuter, V, Scheid, E., Self ignition of Diesel sprays and its dependence on fuel properties and injection parameters, J. of Eng. For Gas Turbine and Power 110, pp. 399-404, 1988.

Payri, R., García-Oliver, J. M., Bardi, M., & Manin, J. (2012). Fuel temperature influence on diesel sprays in inert and reacting conditions. *Applied Thermal Engineering*, *35*, 185-195

Tables

Table 1: Test conditions summary

[1] The injector temperature T_f = 343 K has been used only in liquid length tests

[2] The ambient density T_g = 7.6 kg/m^3 been used only in liquid length tests

[3] The 0% O2 concentration has been employed in liquid length test and 15% in the lift-off length test

Table 2: Fuel temperature estimated for all the conditions tested. The temperature has been obtained averaging the temperature of the injector measured in the first 3 mm from the injector tip

Table 3: Exponents obtained by the regression with equation (4) to LL results. Together with the data is reported also the value of the R^2 calculated

Table 4: Exponents obtained by the regression with equation (8) to LOL results. Together with the data is reported also the value of the R^2 calculated

Table 5: Exponents obtained by the regression with equation (10) to ignition delay results. Together with the data is reported also the value of the R^2 calculated

Figures

Figure 1: Global view of the test chamber of the test rig

Figure 2: Scheme of the injector dummy employed for the injector temperature measurements

Figure 3: Experimental lay-out employed for liquid length measurement

Figure 4: Experimental lay-out employed for OH radical visualization

Figure 5: Sample of the image processing used for LOL measurement. The image recorded by the camera (a) and the intensity profiles of the two half images (b). The threshold is calculated as half of the leveling level calculated for each image.

Payri, R., García-Oliver, J. M., Bardi, M., & Manin, J. (2012). Fuel temperature influence on diesel sprays in inert and reacting conditions. *Applied Thermal Engineering*, *35*, 185-195

Figure 6: temperature along the injector axis for T_g = 900 K. In dashed line is depicted the coolant temperature T_c and the yellow area represent the averaging length for the determination of the fuel temperature T_f. This part of the injector roughly matches with nozzle sac.

Figure 7: Liquid length versus time for three different values of T_f. P_{rail} = 150 MPa, T_{amb} = 900 K, ρ_{amb}= 22.8 $^{kg}/_{m^3}$.

Figure 8: Effect of the T_c variation over LL_m at different ambient density at P_{rail} = 150 MPa

Figure 9: Effect of the T_c variation over LL_m for different injection pressures at ρ_{amb} = 22.8 $^{kg}/_{m^3}$.

Figure 10: Effect of the T_c variation over LOL for different ambient temperatures at ρ_{amb} = 15.2 $^{kg}/_{m^3}$.

Figure 11: Effect of the T_c variation over LOL for different ambient temperatures at ρ_{amb} = 22.8 $^{kg}/_{m^3}$.

Figure 12: Time evolution of 99.9% digital level percentile of the pixel in the images captured in CH chemiluminescence test. The values plotted are the average of 5 repetitions. In the figure the results obtained for three different injection pressures are compared. T_{amb} = 900 K, ρ_{amb} = 22.8 $^{kg}/_{m^3}$.

Figure 13: Ignition delay calculated for all the tests conditions at $T_f = 293\ K$. In this plot measurements performed at $\rho_{amb} = 45.6\ ^{kg}/_{m^3}$ with the same technique have been added.

Figure 14: Effect of the coolant temperature on the injection delay plotted for the density $\rho_{amb} = 15.2\ kg/m^3$ (a) and $\rho_{\text{amb}} = 15.2\text{kg/m}^3$ (b)

Figure 15: Influence of the ambient density on liquid length. Comparison between experimental results and theoretical predictions at p_{rail}= 150 MPa and T_{amb}= 900 K. In this comparison the cone angle used as input in the model has not been changed for the different ambient density.

Figure 16: Influence of the ambient temperature on LL. Comparison between experimental results and theoretical predictions at p_{rail}= 150 MPa. The model has been tuned with the experimental data at T_{amb} = 900 K and the model predictions at T_{amb}= 820 K have been compared with the experimental data.

Figure 17: Influence of the coolant temperature on liquid length. Comparison between experimental results and theoretical predictions; ρ_{amb} = 22.8 $^{kg}/_{m^3}$, p_{rail}= 150 MPa,

Figure 18: Influence of the coolant temperature on the mixture temperature for the case T_{amb} = 900K. The two dashed lines represent the fuel mass fraction related to the LOL, and the fuel mass fraction in the liquid length region for a sample case: ρ_{amb} = 22.8 $^{kg}/_{m^3}$, p_{rail}= 150 MPa.

Payri, R., García-Oliver, J. M., Bardi, M., & Manin, J. (2012). Fuel temperature influence on diesel sprays in inert and reacting conditions. *Applied Thermal Engineering*, *35*, 185-195

Table 1

Parameters	**Values**	**Units**
Fuel	n-dodecane	-
Orifice diameter	0.09	mm
k-factor	1.5	-
Energizing time	2500	μs
Coolant temperature[1] [T_c]	293 - 318 - 343	K
Gas density[2] [ρ_{amb}]	7.6 - 15.2 - 22.8	kg/m^3
Gas temperature [T_{amb}]	820 - 900	K
Injection pressure [p_{rail}]	50 - 100 - 150	MPa
Oxygen concentration[3]	0 - 15	% (vol.)

Table 2

T_{amb} [K]	**T_c [K]**	**T_f [K]**
820	293	331
820	318	358
820	343	377
900	293	341
900	318	369
900	343	391

Payri, R., García-Oliver, J. M., Bardi, M., & Manin, J. (2012). Fuel temperature influence on diesel sprays in inert and reacting conditions. *Applied Thermal Engineering*, *35*, 185-195

Table 3

Exponents	a	b	c	d	e	R^2 [%]
Values	0.5	0.61	1.7	0.61	0.11	99.18

Table 4

Exponents	a	b	c	d	R^2 [%]
Theory	-3.7	-0.8	1	0	-
Adjusted	-3.97	-0.93	0.52	-0.32	99.16

Table 5

Exponents	n	A	m	a	R^2 [%]
Literature	-0.89	2811	-0.14	0	81.5
Adjusted	-0.89	5790	-0.45	-0.38	98.85

Payri, R., García-Oliver, J. M., Bardi, M., & Manin, J. (2012). Fuel temperature influence on diesel sprays in inert and reacting conditions. *Applied Thermal Engineering*, *35*, 185-195

Fig 1

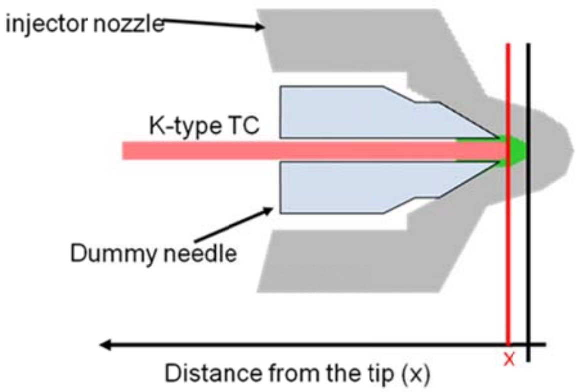

Fig 2

Payri, R., García-Oliver, J. M., Bardi, M., & Manin, J. (2012). Fuel temperature influence on diesel sprays in inert and reacting conditions. *Applied Thermal Engineering*, *35*, 185-195

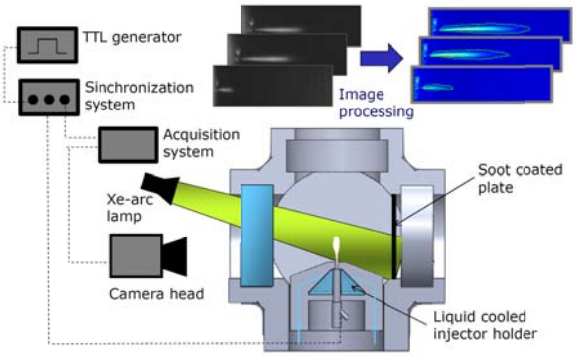

Fig 3

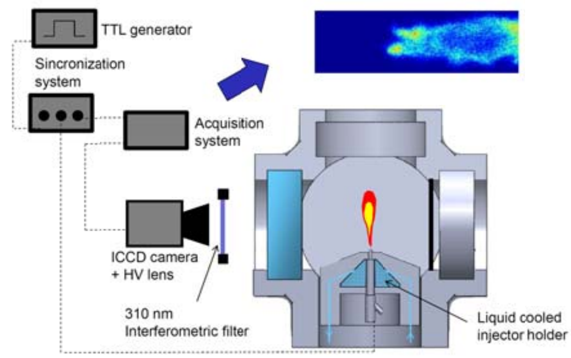

Fig 4

Payri, R., García-Oliver, J. M., Bardi, M., & Manin, J. (2012). Fuel temperature influence on diesel sprays in inert and reacting conditions. *Applied Thermal Engineering*, *35*, 185-195

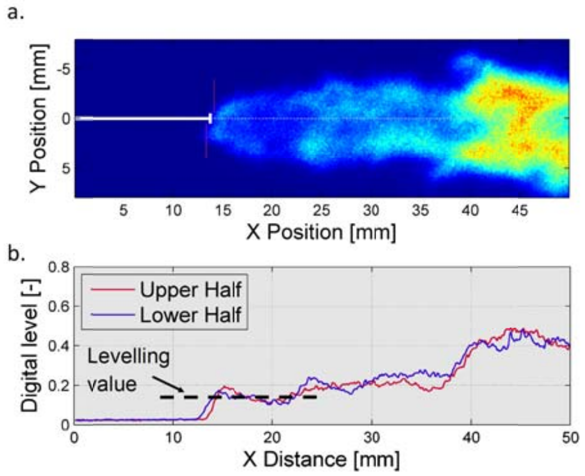

Fig 5

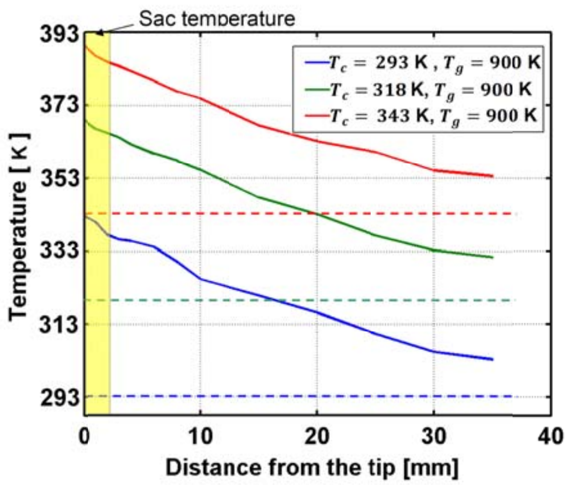

Fig 6

Payri, R., García-Oliver, J. M., Bardi, M., & Manin, J. (2012). Fuel temperature influence on diesel sprays in inert and reacting conditions. *Applied Thermal Engineering*, *35*, 185-195

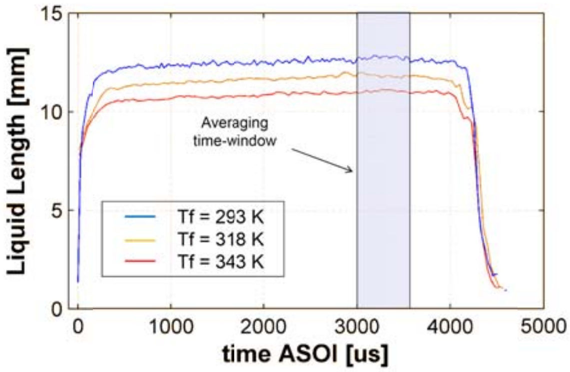

Fig 7

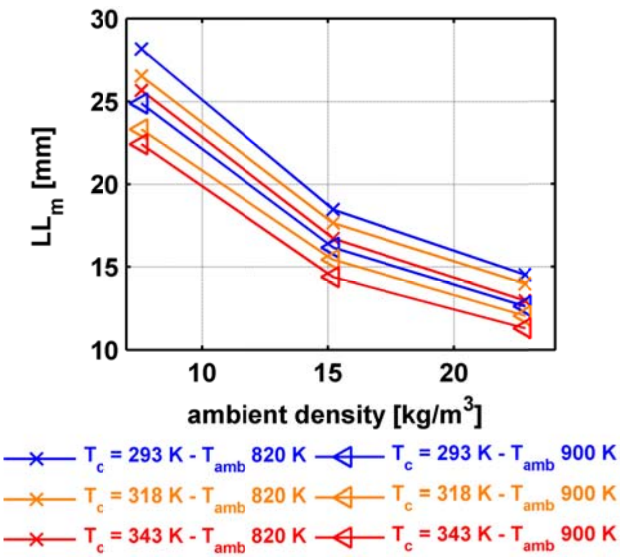

Fig 8

Payri, R., García-Oliver, J. M., Bardi, M., & Manin, J. (2012). Fuel temperature influence on diesel sprays in inert and reacting conditions. *Applied Thermal Engineering*, *35*, 185-195

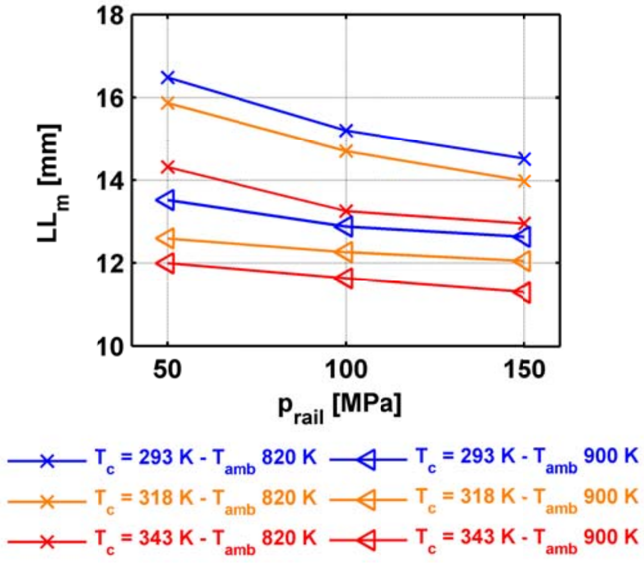

Fig 9

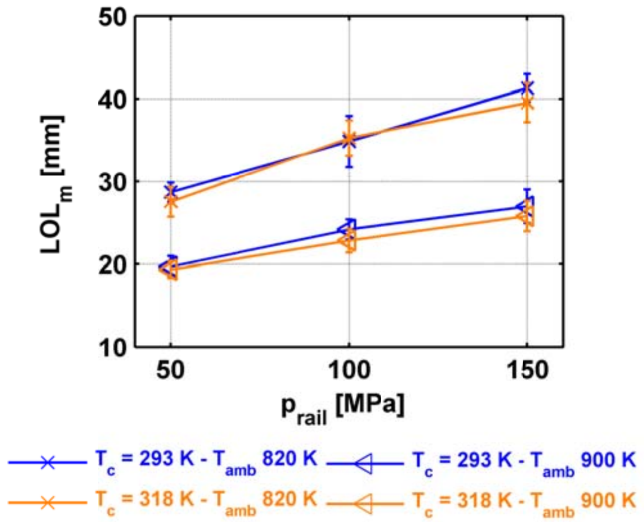

Fig 10

Payri, R., García-Oliver, J. M., Bardi, M., & Manin, J. (2012). Fuel temperature influence on diesel sprays in inert and reacting conditions. *Applied Thermal Engineering*, *35*, 185-195

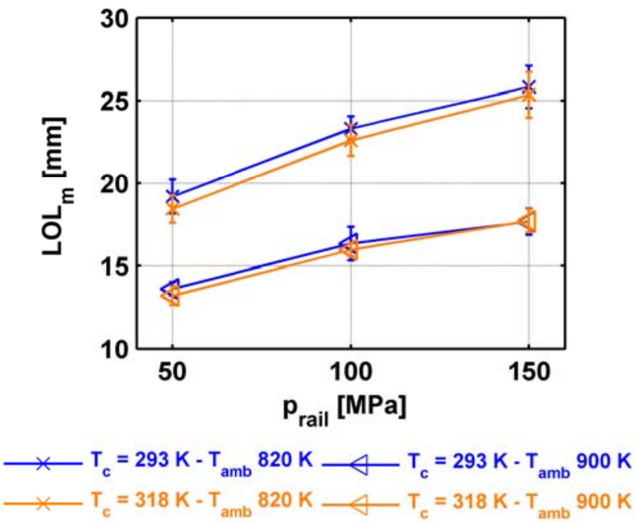

Fig 11

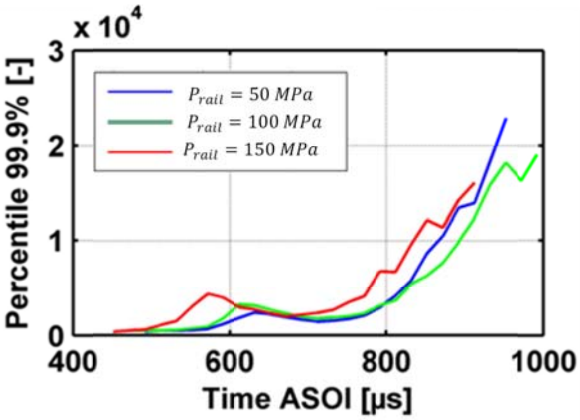

Fig 12

Payri, R., García-Oliver, J. M., Bardi, M., & Manin, J. (2012). Fuel temperature influence on diesel sprays in inert and reacting conditions. *Applied Thermal Engineering*, *35*, 185-195

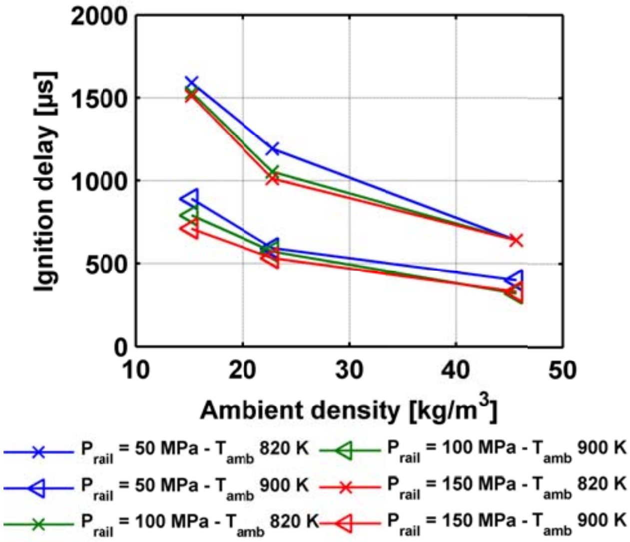

Fig 13

Payri, R., García-Oliver, J. M., Bardi, M., & Manin, J. (2012). Fuel temperature influence on diesel sprays in inert and reacting conditions. *Applied Thermal Engineering*, *35*, 185-195

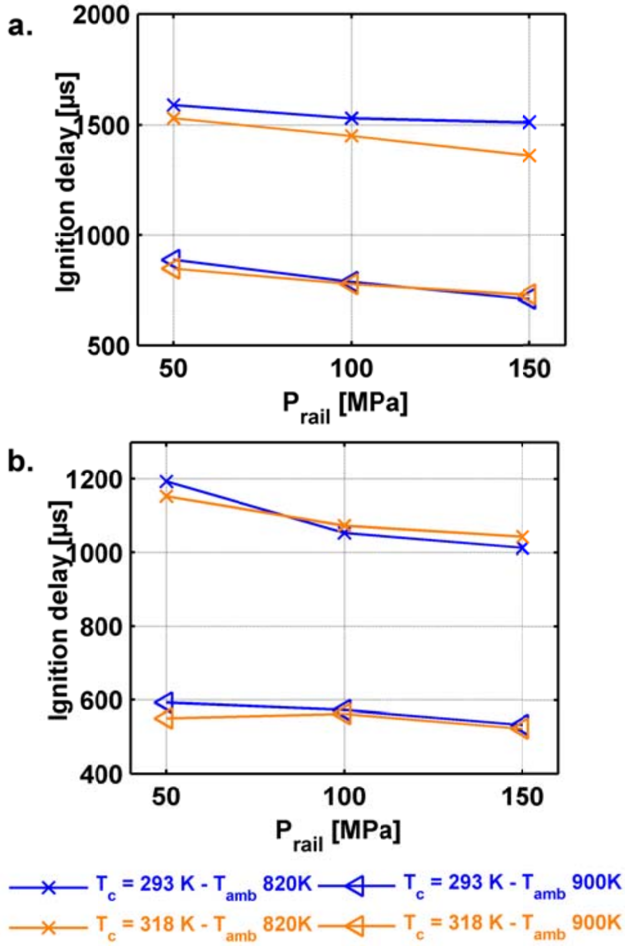

Fig 14

Payri, R., García-Oliver, J. M., Bardi, M., & Manin, J. (2012). Fuel temperature influence on diesel sprays in inert and reacting conditions. *Applied Thermal Engineering*, *35*, 185-195

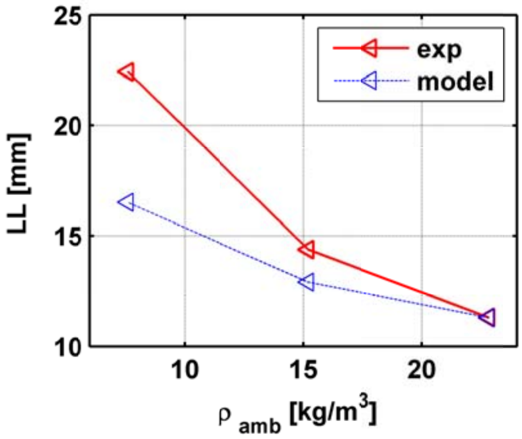

Fig 15

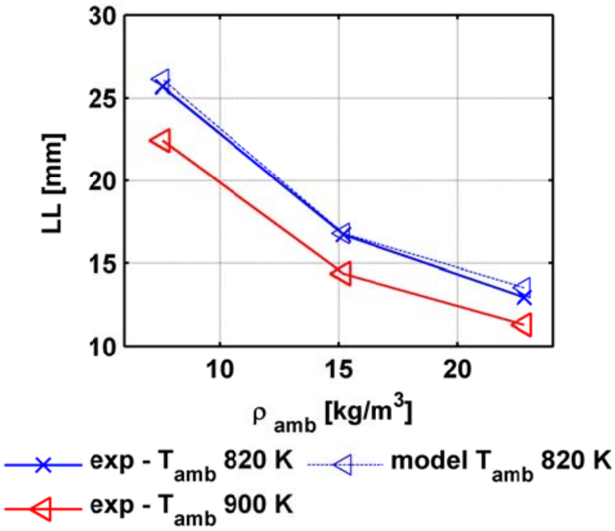

Fig 16

Payri, R., García-Oliver, J. M., Bardi, M., & Manin, J. (2012). Fuel temperature influence on diesel sprays in inert and reacting conditions. *Applied Thermal Engineering*, *35*, 185-195

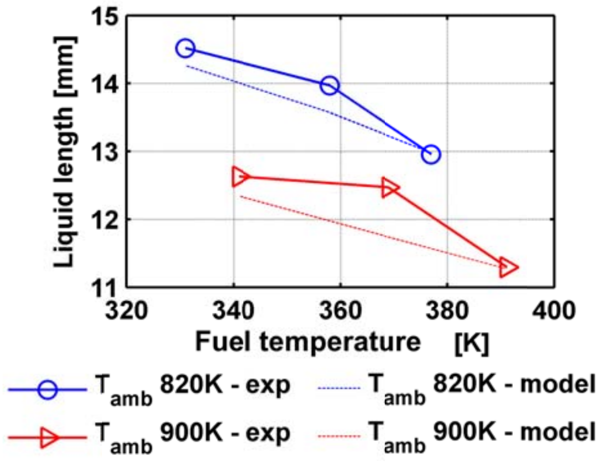

Fig 17

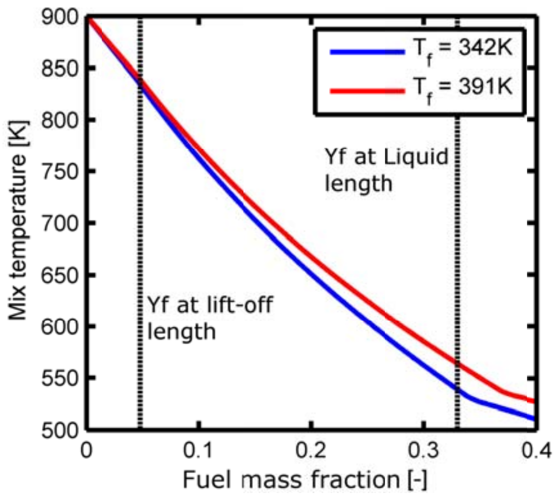

Fig 18